



**HAL**  
open science

## Modeling the effects of farming practices on bovine respiratory disease in a multi-batch cattle fattening farm

Baptiste Sorin-Dupont, Sebastien Picault, Bart Pardon, Pauline Ezanno,  
Sebastien Assié

### ► To cite this version:

Baptiste Sorin-Dupont, Sebastien Picault, Bart Pardon, Pauline Ezanno, Sebastien Assié. Modeling the effects of farming practices on bovine respiratory disease in a multi-batch cattle fattening farm. Preventive Veterinary Medicine, 2023, 219, pp.106009. 10.1016/j.prevetmed.2023.106009 . hal-04276456

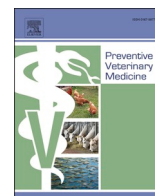
**HAL Id: hal-04276456**

**<https://hal.science/hal-04276456>**

Submitted on 5 Dec 2023

**HAL** is a multi-disciplinary open access archive for the deposit and dissemination of scientific research documents, whether they are published or not. The documents may come from teaching and research institutions in France or abroad, or from public or private research centers.

L'archive ouverte pluridisciplinaire **HAL**, est destinée au dépôt et à la diffusion de documents scientifiques de niveau recherche, publiés ou non, émanant des établissements d'enseignement et de recherche français ou étrangers, des laboratoires publics ou privés.



# Modeling the effects of farming practices on bovine respiratory disease in a multi-batch cattle fattening farm

Baptiste Sorin-Dupont<sup>a,\*</sup>, Sebastien Picault<sup>a</sup>, Bart Pardon<sup>b</sup>, Pauline Ezanno<sup>a,1</sup>,  
Sebastien Assié<sup>a,1</sup>

<sup>a</sup> Oniris, INRAE, BIOEPAR, 44300, Nantes, France

<sup>b</sup> Department of Internal Medicine, Reproduction and Population Medicine, Faculty of Veterinary Medicine, Ghent University, Salisburylaan 133, 9820 Merelbeke, Belgium

## ARTICLE INFO

### Keywords:

Epidemiology  
Stochastic modeling  
Bovine respiratory disease

## ABSTRACT

Bovine Respiratory Disease (BRD) affects young bulls, causing animal welfare and health concerns as well as economical costs. BRD is caused by an array of viruses and bacteria and also by environmental and abiotic factors. How farming practices influence the spread of these causal pathogens remains unclear. Our goal was to assess the impact of zootechnical practices on the spread of three causal agents of BRD, namely the bovine respiratory syncytial virus (BRSV), Mannheimia haemolytica and Mycoplasma bovis. In that extent, we used an individual based stochastic mechanistic model monitoring risk factors, infectious processes, detection and treatment in a farm possibly featuring several batches simultaneously. The model was calibrated with three sets of parameters relative to each of the three pathogens using data extracted from literature. Separated batches were found to be more effective than a unique large one for reducing the spread of pathogens, especially for BRSV and M.bovis. Moreover, it was found that allocating high risk and low risk individuals into separated batches participated in reducing cumulative incidence, epidemic peaks and antimicrobial usage, especially for M. bovis. These findings rise interrogations on the optimal farming practices in order to limit BRD occurrence and pave the way to models featuring coinfections and collective treatments p { line-height: 115%; margin-bottom: 0.25 cm; background: transparent}a:link { color: #000080; text-decoration: underline}a.cjk:link { so-language: zxx}a.ctl:link { solanguage: zxx}

## 1. Introduction

Bovine Respiratory Disease (BRD) is considered a worldwide economic and sanitary burden in the cattle industry (Babcock et al., 2009; Delabouglise et al., 2017). It has been estimated that the cost of BRD could represent up to 20% of the farmers' income in France and up to 44% in North America (Bareille et al., 2009; Mijar et al., 2023). Despite many efforts being made in the prevention and treatment of BRD, both morbidity and mortality have increased over the past 20 years (Hilton, 2014; Blakebrough-Hall et al., 2022).

BRD is a disease of the lower respiratory tract of cattle. It is a multipathogen disease caused by bacteria, viruses and also by abiotic and environmental factors like stress or transportation (Kudirkiene et al., 2021; Assié et al., 2009). Commingling is also outlined as a major risk factor, especially in big herds, as seen in the North American systems

(Mijar et al., 2023). BRD is enhanced by compromised host immune systems and environmental factors (Grissett et al., 2015). In Europe, the most common bacteria associated with BRD complex are *Mycoplasma bovis*, *Mannheimia haemolytica*, *Pasteurella multocida*. Bovine Respiratory Syncytial Virus (BRSV), and parainfluenza virus type 3 (PI3) are the viral agents most frequently reported as pathogenic (Grissett et al., 2015). Each agent has features leading to different pathogenesis (Gershwin et al., 2015). However, BRD clinical signs, which include lethargy, cough, nasal discharge, are not specific to any causal agent of BRD (Griffin, 2010). Consequently, the causative pathogen is generally not precisely identified in the event of an outbreak on farm, even though the difference of efficacy of certain control measures can differ according to the pathogen (Griffin, 2014; Ollivett, 2020).

The cattle production system is still heavily reliant on antimicrobial use (AMU) to control BRD spread (Ollivett, 2020). Without a reliable

\* Corresponding author.

E-mail address: [baptiste.sorin@inrae.fr](mailto:baptiste.sorin@inrae.fr) (B. Sorin-Dupont).

<sup>1</sup> Equal contributions

detection method and pathogen identification, antibiotics are administered based on the appraisal of severe clinical signs (Ives et al., 2015). This method leads to a massive AMU, which efficacy and consequences on antimicrobial resistance are currently questioned (Coetzee et al., 2019). To this day, there is no alternative method proposing more targeted collective treatments, even though the general overuse of antibiotics is a growing concern worldwide as it is thought to decrease treatment efficiency (Laxminarayan et al., 2013).

In addition, the individual risk of contracting BRD, and subsequently spreading it, is heterogeneous among animals upon arrival in the fattening farms (Poizat et al., 2019). Environmental factors increasing the probability of BRD onset include stress, weaning, poor sanitary situation of the breeding farms (Grissett et al., 2015; Cernicchiaro et al., 2012). In Europe, most young bulls from beef breeds are produced by cow/calf breeders and fattened by specialized fatteners (Poizat et al., 2019). After weaning, young bulls are transported to sorting facilities and sorted in batches by bodyweight, then shipped to the fatteners. However, the individual exposure to factors inducing BRD is not taken into account when forming pens (Poizat et al., 2019). Conversely, in Anglo-Saxon systems, risk level assessment and preconditioning programs of high-risk animals are implemented, albeit not systematic (Hay et al., 2014, 2016). Taking individual risk factors into consideration when composing batches could influence young bulls' health on feedlots (Herve et al., 2020). However, whether the batches should be homogeneous or not in terms of individual risk level has not been questioned yet.

Mechanistic models simulating the spread of pathogens in diversified conditions could allow ranking possible interventions. Indeed, they could allow quantifying their impact on the circulation of the pathogens involved in BRD and on the general impact of the disease. Moreover, including stochasticity in the models could account for variability in the biological processes, the random events and the parameter uncertainty. Modeling is used to understand complex infection dynamics and compare scenarios and interventions (Ferguson et al., 2005; Keeling, 2005). In the case of BRD, a model describing mathematical equilibria in a BRSV epidemic has been published (Greenhalgh et al., 2009). Models ranking interventions and zootechnical practices at pen level have also been published (Picault et al., 2019; Picault et al., 2022). They simulated the circulation of an average pathogen in conditions mimicking contrasted farming contexts such as small versus large batches (considered isolated). They concluded on a bigger BRD circulation in large pens composed of high risk individuals. Risk factors were also used in predictive tools showing limited success (Babcock et al., 2013; Amrine et al., 2019). However, no model combining pathogen specific dynamics with scenario ranking on zootechnical interventions at batch scale has been proposed yet.

Our objective was to use stochastic simulations to evaluate three farm management practices on the spread of different pathogens involved in BRD. More specifically, we tested three batch allocation systems (*i.e.* sorted, homogenous, unique) in two distinct proportions of individual risk level. We then compared the outcomes of these scenarios in terms of disease occurrence and AMU, to outline the best scenario. To that extent, we developed a multibatch stochastic individual-based mechanistic model of the on-farm spread of pathogens involved in BRD occurrence. We then used it to simulate the cumulative incidence, the height of the epidemic peak and the AMU for each pathogen in every scenario.

## 2. Materials and methods

### 2.1. BRD model: processes and assumptions

We proposed to model the spread of BRSV, *M. haemolytica*, and *M. bovis*. BRSV is a highly infectious airborne virus, *M. bovis* is a contact spreading long-time persisting primary agent and *M. haemolytica* is an opportunistic pathogen. These pathogens have distinct infectious

dynamics and are the most pathogenic representatives of the three different groups of pathogens frequently involved in BRD: respiratory viruses, Pasteurellaceae, and mycoplasmas, respectively.

We implemented an original stochastic mechanistic individual-based model calibrated with one of three sets of parameters relative to each of the three considered pathogens. This model was developed with the framework EMULSION (Picault et al., 2019). This open-source framework describes the models as human-readable structured text files, processed by a generic simulation engine written in Python. This structure could allow infectious disease modelers, computer and animal scientists to discuss and to revise the model at any time without writing any code. This framework also bears the advantage of enabling individual-based stochastic modeling, which is useful when modeling small groups with high variability. This framework fosters a decomposition of the modeled events and processes. Processes were described as finite state machines, a formalism broadly used in computer science to represent states and transitions, and able to encompass flow diagrams more classically used in epidemiological modeling.

The model extended a previously published model enabling pathogen transmission in a building containing several batches, *i.e.* groups of animals sharing a same closed indoor space (Sorin et al., 2022). We model the situation as all-in all-out: calves of the same batch arrive at the same time, stay together and leave the farm at the same time. This structure allows accounting for the between-batch transmission within a given building in the first few weeks of fattening operations. The model was in discrete time with time steps of 1/2 day. It monitored 6 processes: risk status, hyperthermia, health status, clinical signs, detection, and treatment. Each process had several states, listed in Table 1. The complete equations of the model can be found in SI1. Additionally, a graphical overview is available in SI2.

Risk status defined the individual risk of becoming infected and of shedding pathogens. It was a qualitative information (low, medium, or high) summarizing the level of stressors encountered by the individual prior to its arrival at the feedlot (Cernicchiaro et al., 2012; A. H. Babcock et al., 2013). The higher the risk, the higher the infection rate and the more likely the animals were to shed pathogens if infected. Risk status did not change over time, consequently, there was no equation relative to it.

Hyperthermia was composed of two states: hyperthermic (H) and non-hyperthermic (NH) animals. NH could become H with probability  $p_H$  due to non-infectious causes, and then stayed in H for a duration  $\tau_H$  drawn in a Beta distribution calibrated from observed data, before returning to NH. The transitions from NH to H and then back to NH could also be totally driven by the infection process.

We considered six health statuses: susceptible (S1), asymptomatic carrier (E), first infection (I1), second infection (I2), resistant (R) and partially resistant (S2) animals. The process differed between BRSV and

**Table 1**  
Detailed states of each model process.

Process	State	Abbreviation
Health state	Susceptible	S1
	Asymptomatic carriers	E
	First infection	I1
	Second infection	I2
	Resistant	R
	Partially resistant	S2
Hyperthermia	Non hyperthermic	NH
	Hyperthermic	H
Clinical signs	Asymptomatic	A
	Mild clinical signs	M
	Severe clinical signs	C
	Dead	X
Detection	Detected	D
	Undetected	U
Treatment	Treated	T
	Not treated	NT

the two bacteria. For both bacterial processes, asymptomatic carriers could spontaneously turn I1 with probability  $p_E$  and could also be infected by surrounding infectious individuals (I1). When entering I1 state, three actions were triggered: (1) the individual exhibits mild clinical signs for a duration  $\tau_M$  drawn from a Beta distribution calibrated from observed data, (2) the animal changed from NH to H state, (3) a random sort with probability  $p_C$  drives whether the individual will display severe clinical signs at the end of its mild clinical signs. If displaying severe clinical signs, a boolean deciding on the survival of the individual was drawn from a binomial law of probability  $p_d$ . Death occurred at the end of the severe clinical signs duration ( $\tau_C$ ). If the individual did not die from infection, it then recovered and became resistant (R). Recovery occurred after duration  $\tau_r$  drawn from a gamma distribution according to the given bacterial pathogen. Theoretically,  $\tau_r$  is longer than  $\tau_M$ . However,  $\tau_M + \tau_C$  could exceed  $\tau_r$ . In that case, the infectious period was  $\tau_M + \tau_C$ . Under the assumption that infectious individuals would be detected prior to the arrival on farm, we used E individuals for BRSV to just serve the purpose of introducing future infectious animals in the population. Hence, their probability of subsequently becoming infectious was 1. Phenomena of partial immunity and reinfections are known for BRSV (Sharma and Woldehiwet, 1992; Van der Poel et al., 1993; Hall et al., 1991). We thus considered two susceptible states (S1 and S2) upon arrival on the farm, depending on whether the individual has been exposed to BRSV before or not. Upon infection, S1 would transition to I1 and S2 to I2. To represent partial immunity, S2 were less susceptible than S1 and I2 were less infectious than I1. As for *M. haemolytica* and *M. bovis*, both transitions to an infectious state trigger the transition from NH to H. Both infectious states transition to R at the end of their infectious period. A transition from R to S2 should exist, however the immune period has been shown to be longer than the duration we consider for our simulation, it was thus left out (Klem et al., 2019; Ellis et al., 2013). For every pathogen, when transitioning to R state, animals changed from H to NH.

Two detection methods were used. The first detection relied on visual on-farm appraisal of clinical signs, assuming lethargy was the most significant sign to calibrate the delay ( $\tau_M$ ) between infection and severe sign occurrence. Severe clinical signs were detected with a sensitivity of 1, while the sensitivity for mild clinical signs detection was averaged to 0.5 (Kayser et al., 2019). The model assumed a clinical check-up at every time step (12 h). Following the detection of the first case through visual appraisal, all hyperthermic animals were identified using rectal temperature measured at the next feeding time, 12 h later. Although not systematically practiced in French young bulls' operations, this approach is recommended (Timsit et al., 2011).

Each animal detected as diseased or hyperthermic could transition from not treated (NT) to treated (T). Treated animals received one antibiotic dose, assumed to be effective after a certain duration  $\tau_T$ . If animals still exhibited clinical signs after this duration, they would be treated again for the same duration, but the number of treatments per episode was limited ( $\max_T$ ). The AMU modeled the total number of doses used over the course of a simulation. Transitions from T to NT occurred in three cases: (1) recovery after  $\tau_T$  due to successful treatment with probability  $p_T$ , (2) the end of the infectious period occurred while under treatment but was not caused by it, (3) the animal still showed severe clinical signs but had already been treated the maximum allowed number of times (treatment failure). Despite the absence of curative treatment for viral infections, the treatment process was kept to monitor the antimicrobial use caused by visible clinical signs appraisal due to virus (i.e., when no pathogen identification was performed). However, the treatment success probability was set to zero in such cases.

Force of infection: the force of infection  $\Phi_i$  for batch  $i$  is a frequency-dependent rate. The computation of the force of infection ( $\Phi$ ) takes into account the multi-batch nature of our model by considering the force of infection both within each batch and between batches. Let  $B$  be the set of batches of  $n$  individuals each raised simultaneously in a building. Within each batch  $i$ , the intra-batch force of infection was determined by

summing the individual contribution  $\beta_\rho$  of each infectious ensemble of individual of risk level  $\rho$  ( $I_{\rho,i}$ ). The contribution increased with the individual risk level  $\rho$ . Mathematically, this translates to Eq. (1).

Within a given batch  $i$ , susceptible individuals experienced an intra-batch force of infection with the addition of the contributions of the other batches of set  $B$  deprived of  $i$  ( $B \setminus \{i\}$ ) multiplied by a contact rate between batches denoted as  $c$ . The contact rate determined how isolated the batches were from each other, and ranged from  $c=0$  for perfectly isolated batches to  $c=1$  for no isolation. This total was multiplied by a susceptibility factor  $\sigma_\rho$  increasing with the individual risk level  $\rho$ . Mathematically, this translates to Eq. (2). EMULSION automatically converts the force of infection  $\Phi_i$  to a time-dependent probability  $p_{\Phi_i}$  using the Eq. (3), with  $\delta t$  being the current time step.

$$\forall i \in B, \lambda_i = \sum_{\rho \in P} \beta_\rho I_{\rho,i} \tag{1}$$

$$\Phi_i = \sigma_\rho \left( \frac{\lambda_i + c \sum_{b \in B \setminus \{i\}} \lambda_b}{N_i + c(N - N_i)} \right) \tag{2}$$

$$p_{\Phi_i}(\delta t) = e^{1 - \Phi_i \delta t} \tag{3}$$

with  $P$  the set of individual risk levels,  $\beta_\rho$  the shedding level of individuals with risk level  $\rho$ ,  $I_{\rho,i}$  the number of infectious individuals with risk level  $\rho$  in batch  $i$ ,  $N_i$  the total number of individuals in batch  $i$ ,  $N$  the total population size. This function was proposed for modeling the force of infection as it enables to represent perfectly separated batches ( $c=0$ ) as well as a unique large batch with homogeneous contacts ( $c=1$ ) using a single formula.

### 2.2. Review of individual pathogen characteristics

Key information for building our model were relative to pathogen transmission (rate, probability of spontaneous shedding), duration of clinical signs, infectious period and probability of displaying severe clinical signs. Information on the probability of treatment success was also taken into account. In total, we used data from 16 articles to parameterize our model on BRSV, *M. haemolytica* and *M. bovis*. The parameters are summarized in Tables 2–4.

### 2.3. Scenarios and outputs

We first investigated six scenarios on 200 individuals for 40 days, as BRD typically occurs in the first few weeks of fattening (Assié et al.,

**Table 2**  
Parameter values used for *M. haemolytica*.

Parameter	Symbol	Value	Source
Transmission rate to susceptible (/h)	$\beta$	0.005, 0.008 and 0.012 for low, medium and, high risk levels respectively	(Picault et al., 2022)
Spontaneous shedding probability	$p_E$	0.14, 0.42 and 0.68 for low, medium, and high risk levels respectively	(Frank et al., 1986)
Initial carrier proportion	$E_0/N_0$	0.26, 0.48 and 0.72 for low, medium, and high risk levels respectively	(Timsit et al., 2013)
Mild clinical sign duration	$\tau_M$	2–8 (med=6) days	(Grissett et al., 2015)
Infectious period duration	$\tau_I$	6–10 (med=8) days	(Thomas et al., 2019)
Asymptomatic period duration	$\tau_E$	1 day	(Grissett et al., 2015)
Probability of successful treatment	$p_T$	0.71	(DeDonder, Apley, 2015)
Probability of severe forms	$p_C$	0.65	(Timsit et al., 2013)

**Table 3**  
Parameters used for BRSV.

Parameter	Symbol	Value	Source
$R_0$	$R_0$	36.5	(Chase, 2021)
Reduction factor of the susceptibility for second infection	$\psi$	0.25	(Hall et al., 1991)
Reduction factor of the infectiousness for reinfected (I2) individuals	$\chi$	0.126	From (Hall et al., 1991; Chase, 2021)
Reproduction ratio in an endemic situation	$R$	1.14	(Chase, 2021)
Transmission rate (/h)	$\beta$	0.178, 0.238 and 0.297 for low, medium, and high risk levels respectively	From (Chase, 2021; De Jong et al., 1996)
Spontaneous shedding probability	$p_E$	1	(Tjørnehøj et al., 2003)
Initial proportion of partially immune	$S_{20}/N_0$	0.78, 0.63 and 0.47 for low, medium, and high risk level respectively	(Sacco et al., 2014; Wolff et al., 2015)
Initial carrier proportion	$E_0/N_0$	0.06, 0.122 and 0.181 for low, medium, and high risk level respectively	(Assié et al., 2009)
Mild clinical sign duration	$\tau_M$	2–10 (med=5) days	(Grissett et al., 2015)
Infectious period duration	$\tau_I$	4–8 (med=6) days	(Grissett et al., 2015)
Asymptomatic period duration	$\tau_E$	2–5 (med=3) days	(Grissett et al., 2015)
Probability of successful treatment	$p_T$	0	
Probability of severe forms	$p_C$	0.6	(Brodersen, 2010)

**Table 4**  
Parameter values used for M. bovis.

Parameter	Symbol	Value	Source
Transmission rate to susceptible (/h)	$\beta$	0.005, 0.008 and 0.012 for low, medium, and high risk levels respectively	(Picault et al., 2022)
Spontaneous shedding probability	$p_E$	0.65, 0.8 and 1 for low, medium, and high risk levels respectively	(White et al., 2012)
Initial prevalence	$E_0/N_0$	0.094, 0.4 and 0.6 for low, medium, and high risk level respectively	(Caswell et al., 2010; Le Grand et al., 2008; Nobrega et al., 2021)
Mild clinical sign duration	$\tau_M$	5–13 (med=8) days	(Grissett et al., 2015)
Infectious period duration	$\tau_I$	14–28 (med=21) days	(Grissett et al., 2015)
Asymptomatic period duration	$\tau_E$	1–5 (med=2) days	(Grissett et al., 2015)
Probability of successful treatment	$p_T$	0.6	(Caswell et al., 2010)
Probability of severe forms	$p_C$	0.23	(White et al., 2012)

2009; Timsit et al., 2013). These scenarios combined three ways of organizing a building and two distributions of individual risk levels. The building could either be organized with a unique large batch of 200 (unique), 10 batches of 20 with equal proportions of animals among the three individual risk levels (homogeneous) or 10 batches sorted by risk levels (sorted). Risk level proportion (RLP) were either 30%, 40%, and 30% of low, medium, and high risk respectively (HR30) or 90%, 0% and 10% of low, medium and high risk respectively (HR10) (Amrine et al., 2019). Each scenario had 200 stochastic replicates.

We observed the average number of infectious individuals in each batch. At farm scale, we observed the median number of infectious individuals at the epidemic peak, the average number of infectious individuals over time, as well as the cumulative incidence, *i.e.* the sum of transition to an infectious state over the course of the simulation. We also computed a false negative rate by dividing the total number of undetected cases by the cumulative incidence. Moreover, we calculated the total AMU in the farm. Finally, we counted the median number of batches with at least one infectious animal. We then compared the outputs from every scenario. The outputs were mostly counts and normality could not be verified. Moreover, most comparisons had more than two groups with heterogeneous variance. In these conditions, we limited our analysis to the observation of trends in the distributions, and the comparison of medians.

2.4. Sensitivity analysis

To better understand the behavior of the model and to characterize the impact of parameter uncertainty, we carried out an exploration of the model sensitivity by performing sensitivity analysis on three scenarios per pathogen with a common RLP of 30%, 40% and 30% of low risk, medium risk and high risk respectively. The first scenario was HR30-homogeneous, *i.e.* 10 batches of 20 with equal proportions of animals among the three individual risk level. The second was HR30-sorted, *i.e.* 10 batches of 20 animals sorted by risk levels. The third scenario was HR30-unique, *i.e.* one large batch of 200 animals.

This sensitivity analysis incorporated all the parameters involved in processes such as infection, detection, clinical signs and treatment. We also incorporated parameters tuning the initial conditions. The sensitivity analysis targeted 5 model outputs: detection peak height, infection peak height, cumulative incidence, AMU and false negative rate. Each model parameter was used at its nominal value and with a variation of  $\pm 20\%$  (with a [0,1] bound for probabilities). The parameters used during the analysis as well as the corresponding symbol they refer to in the equations are listed in Table 5. Each 19 parameter had 3 possible values, so a complete factorial design incorporating first-order parameter interactions would feature  $3^{19}$  possible combinations of parameter values. For reasons of computational cost and time, we used a fractional factorial design using the R library “planor”. This library allows an optimal space exploration and factorial design generation based on quasi-Monte Carlo methods (Kobilinsky et al., 2017) (hence, reducing the  $3^{19}$  possible combinations of parameter values to  $3^8 = 6561$  parameter settings per scenario).

For each parameter setting, we conducted 200 runs, enabling us to compute an average value for every considered output in every parameter combination. We then employed a standard procedure for sensitivity analysis (Saltelli et al., 2010). For each scenario, an analysis of variance (ANOVA) was performed to identify the sensitivity index, *i.e.* the contribution of model parameters to the variance of the outputs. Outputs whose distributions did not comply with the assumptions of the ANOVA were discarded.

For each output, a linear regression model was fitted with the principal effects of the parameters and their first-order interactions. The contribution of parameter  $p$  to the variation of output  $o$  is calculated as described in Eq. 4, where  $SS_{tot}^o$ ,  $SS_p^o$  and  $SS_{p:p'}^o$  are, respectively, the total sum of squares of the model, the sum of squares related to the principal effect of parameter  $p$ , and the sum of squares related to the interaction between parameters  $p$  and  $p'$ , for output  $o$ .

$$C_p^o = \left( \frac{SS_p^o + \sum_{p'} SS_{p:p'}^o}{SS_{tot}^o} \right) \tag{4}$$

2.5. Analysis of the interbatch contact rate effect

To characterize how the impact of the contact rate between batches

**Table 5**

Overview of the parameters scaled during the sensitivity analysis. The nominal values of the pathogen specific parameters are listed in Tables 2 to 4.

Sensitivity analysis parameter name	Symbol	Role	Nominal value	Source
p_death	$p_D$	Probability that an animal with severe clinical signs eventually dies from BRD	0.05	(Picault et al., 2022)
dur_before_death	$\tau_C$	Duration of severe clinical signs before death for animals dying from BRD (h)	$10 * 24$	(Picault et al., 2019)
dur_I	$\tau_I$	Infection duration	Tables 2–4	Tables 2–4
reactivation	$p_E$	Probability of spontaneous shedding	Tables 2–4	Tables 2–4
dure_E	$\tau_E$	Duration in E state	Tables 2–4	Tables 2–4
transmission_lowrisk	$\beta_{LR}$	Transmission rate of low risk individuals	Tables 2–4	Tables 2–4
transmission_mediumrisk	$\beta_{MR}$	Transmission rate of medium risk individuals	Tables 2–4	Tables 2–4
transmission_highrisk	$\beta_{HR}$	Transmission rate of high risk individuals	Tables 2–4	Tables 2–4
interbatch_contact_rate	c	contact rate between batches	0.01	Assumed
p_detection	$p_{CD}$	Probability of detecting severe clinical signs	1	Assumed
Se_MildC	$p_{MD}$	Probability of detecting mild clinical signs	0.5	(Kayser et al., 2019)
partial_immunity_factor	$\psi$	Partial immunity for S2 individuals (BRSV only)	0.25	Table 3
shedding_reduction_factor	$\chi$	Factor reducing infectiousness for I2 individuals (BRSV only)	0.126	Table 3
sensitivity_lowrisk	$\sigma_{LR}$	Sensitivity factor for low risk susceptible individuals	1	Assumed
sensitivity_mediumrisk	$\sigma_{MR}$	Sensitivity factor for medium risk susceptible individuals	1.5	Assumed
sensitivity_highrisk	$\sigma_{HR}$	Sensitivity factor for high risk susceptible individuals	2	Assumed
proportion_carrier_low	$E_{LR,0}/N_0$	Initial proportion of low risk carriers	Tables 2–4	Tables 2–4
proportion_carrier_medium	$E_{MR,0}/N_0$	Initial proportion of medium risk carriers	Tables 2–4	Tables 2–4
proportion_carrier_high	$E_{HR,0}/N_0$	Initial proportion of high risk carriers	Tables 2–4	Tables 2–4

(c) on epidemiological dynamics could vary among scenarios with contrasted populations, we explored the sensitivity of three model outputs to the parameter value. The considered outputs were the cumulative incidence, the detection peak height and the number of diseased batches. After a preliminary analysis, the range of the contact rate was set between 0 and 0.2 by steps of 0.004 (50 tested values). When the contact rate was superior to this value, there was no difference between the scenarios. We conducted 200 runs for each value of the contact rate on two scenarios: HR10-homogeneous and HR10-sorted. These scenarios were chosen as HR10-sorted only has one high-risk batch, which

was thought to yield enhanced contrast with HR10-homogeneous. For each considered output, we computed its median value as well as its quartiles across the range of the runs.

### 3. Results

#### 3.1. Batch scale

The spread of every pathogen was stratified in batches composed of animals sorted according to their individual risk level (Fig. 1, top rows).

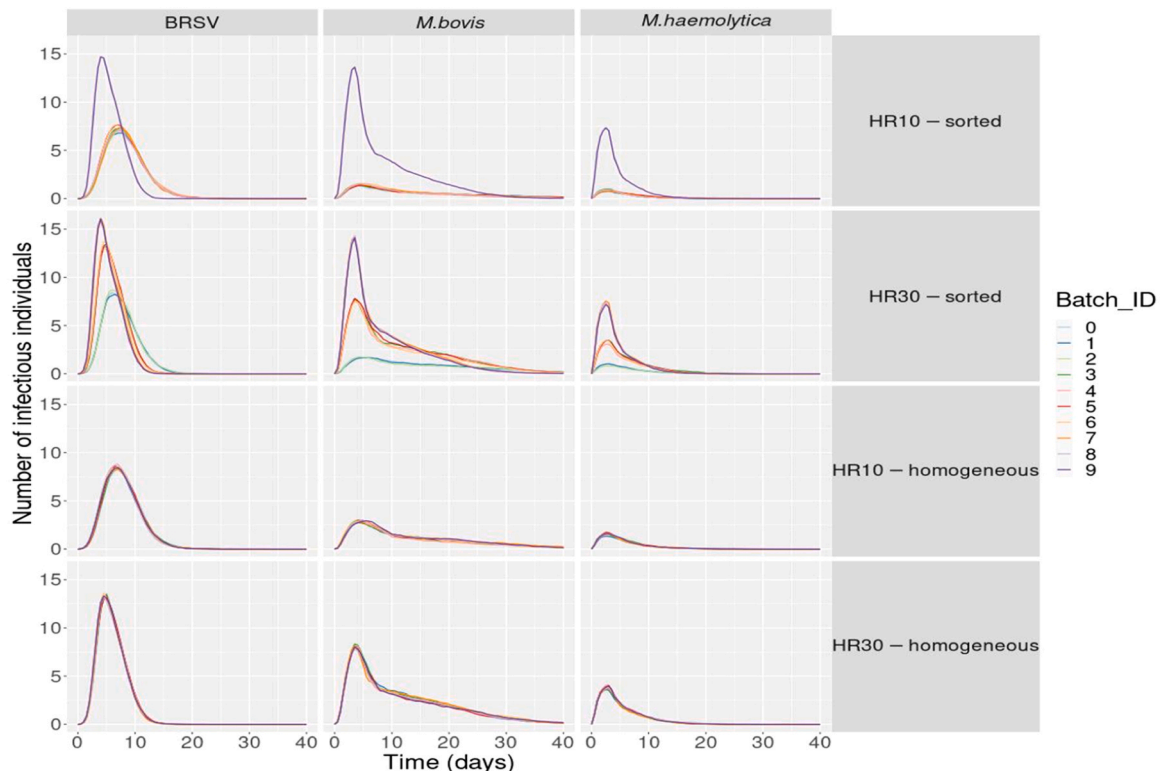


**Fig. 1.** Average number of infected individuals in each batch over time. In column: pathogens. First row: batches 0–8 are entirely composed of low risk individuals and batch 9 is composed exclusively of high risk individuals (HR10-sorted). Second row: batches 0–2 are composed of low risk level individuals, batches 3–6 are composed of medium risk individuals and batches 7–9 are composed only of high risk individuals (HR30-sorted). Third row: 10 batches with equal proportions of 90%, 0% and 10% of low, medium, and high risk individuals respectively (HR10-homogeneous). Fourth row: 10 batches with equal proportions of 30, 40, 30% of low, medium, and high risk individuals respectively (HR30-homogeneous).

It remained stratified when the RLP was changed. Indeed, in Fig. 1 we observed a similar pattern in high and low risk batches between the HR30 and the HR10.

Batches with higher proportions of high risk individuals had a higher epidemic peak than medium or low risk batches. For BRSV, they also had shorter extinction times than medium or low risk batches. We also observed a delay in the peaks when the risk level decreased.

Conversely, we observed that all batches behaved similarly in scenarios with homogeneous risk levels. Additionally, in scenarios with homogeneous risk levels, increasing the proportion of low risk individuals led to a decrease in the height of the infectious peak in every batch.

### 3.2. Farm scale

At farm scale, the scenarios with a larger proportion of low-risk individuals (HR10) showed a lower median epidemic peak than the scenarios with balanced risk proportions (HR30) for every pathogen (Fig. 2). The scenarios with batches sorted by risk levels (in orange) exhibited lower median heights of the epidemic peak than scenarios with homogeneous composition (in green) and the scenario with a unique batch (in blue) in both RLP for BRSV. Conversely, for *M. haemolytica* and *M. bovis*, we observed no noticeable differences between the distributions along the scenarios.

At farm scale, the scenarios showed similar trends in the shape of the epidemic peaks for BRSV and *M. haemolytica* while contrasting dynamics were observed for *M. bovis* (Fig. 3). Indeed, the unique scenario resulted in longer persistence in both RLP. For every pathogen, every scenario produced higher peaks when the proportion of high risk individuals was increased.

At comparable RLP for *M. bovis* and *M. haemolytica*, the sorted and homogeneous scenarios showed similar dynamics, with lower

persistence for the sorted scenario. However, for *M. bovis*, the scenario with a unique batch showcased a rebound of the infected proportion after the epidemic peak. The amplitude of this rebound was increased when the high risk proportion was increased. This rebound was also observable with *M. haemolytica*, but with a less pronounced amplitude.

The scenarios with lower proportions of high risk individuals showed lower farm-scale cumulative incidence for every pathogen (Fig. 4). *M. bovis* exhibited the most contrast between the scenarios, with a lower median of the distribution for the sorted scenario. The sorted scenario also demonstrated a lower median cumulative incidence for BRSV, although the overlap of the distributions was more important. Conversely, having a unique batch either had no significance (for BRSV and *M. haemolytica*, at HR30) or yielded a higher median cumulative incidence (*M. bovis* at HR10 and HR30).

The false negative rates were also impacted by the farming practices and RLP, especially for *M. bovis* (Fig. 5). Indeed, in both RLP, the median false negative rate was higher in the unique batch scenario than for the other two scenarios. However, the median false negative rate for the unique batch scenario decreased when the proportion of high risk was decreased, even though the variances were not equal between these distributions. Conversely, the distributions of the sorted and homogeneous scenarios did not display any noticeable differences. For BRSV and *M. haemolytica*, no noticeable trends in the distributions of the false negative rate were observable.

The AMU displayed contrasts similar to the cumulative incidence (Fig. 6). The AMU was particularly high (a median of more than one dose/individual) for BRSV. The AMU was lower for HR10 scenarios than for their HR30 counterparts. Additionally, with comparable RLP, the median AMU was the lowest in sorted scenarios for *M. bovis*.

The scenarios with sorted batches yielded a lower median number of diseased batches than the homogeneous scenario for *M. bovis* and *M. haemolytica*, especially in HR10 populations (Fig. 7). As the unique

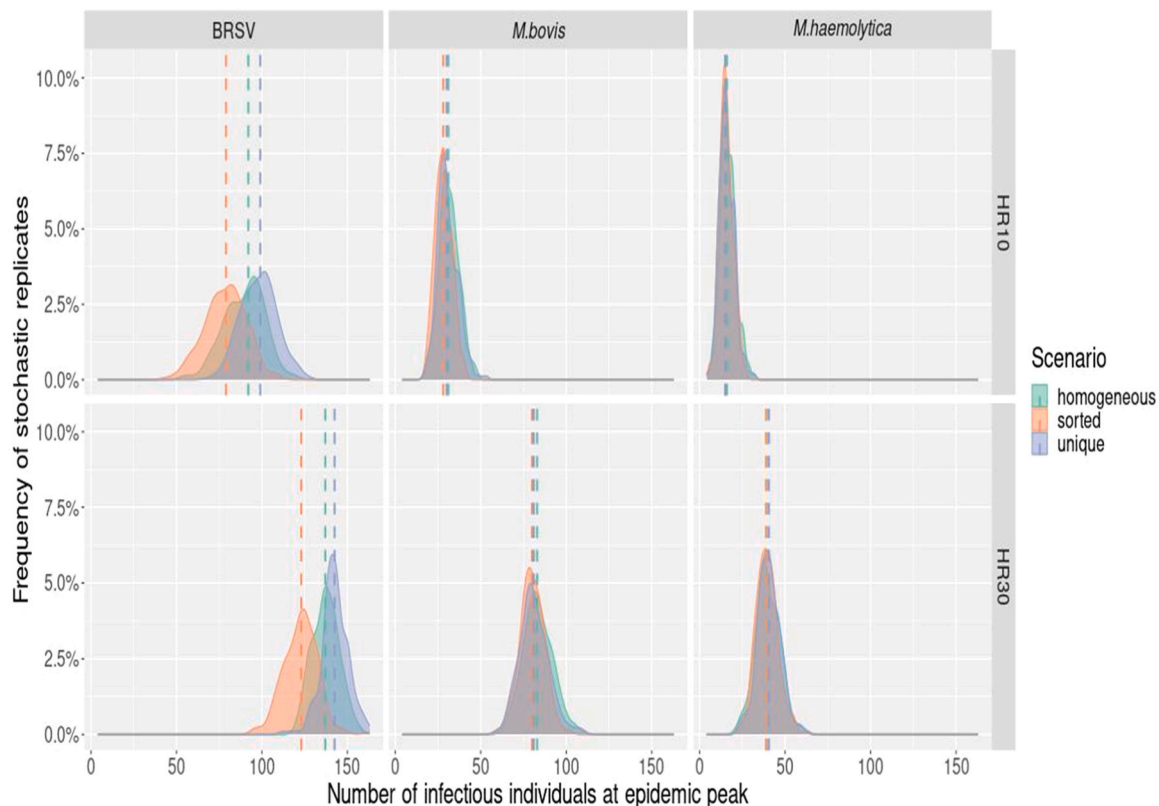


**Fig. 2.** Distributions of the height of the infectious peak at farm scale for each pathogen and scenarios. HR30: 30%, 40% and 30% of low, medium, and high risk level respectively. HR10: 90% of low risk individuals and 10% of high risk. Homogeneous: all 10 batches have equal risk level proportions. Sorted: each one of the 10 batches is composed of only one risk level. Unique: there is only one batch.

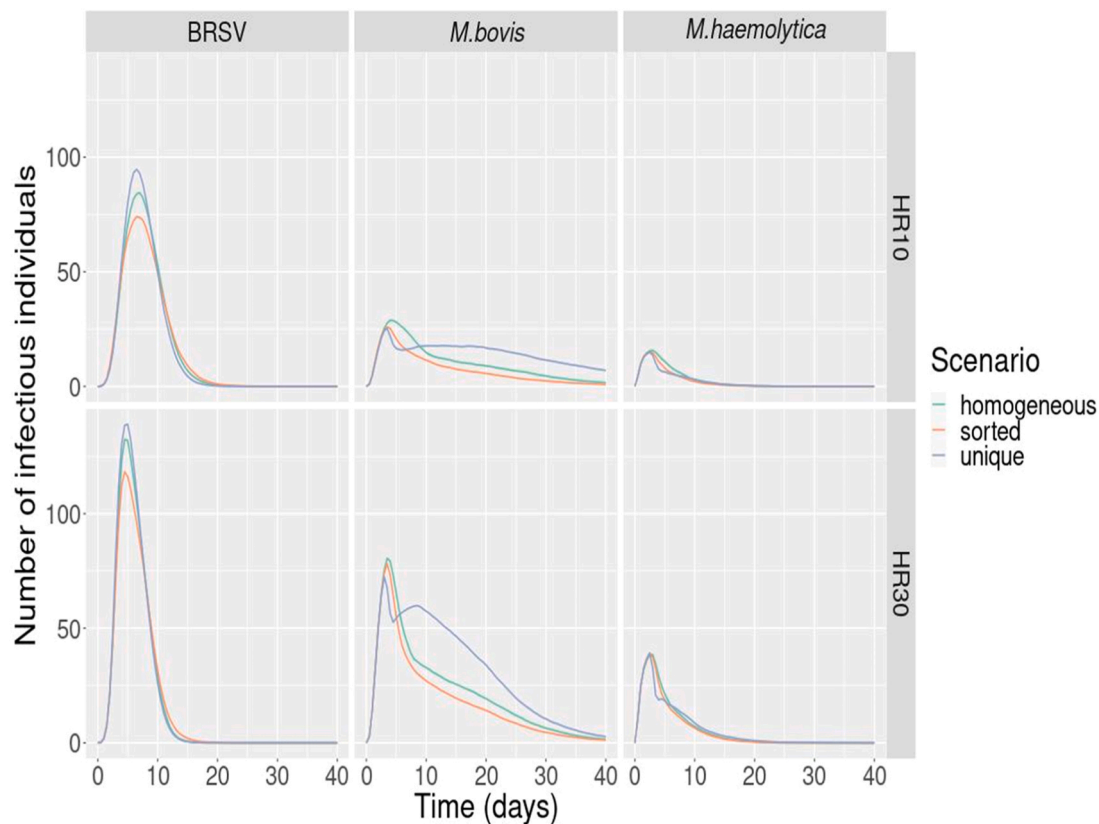


**Fig. 3.** Impact of the scenario on the average proportion of infected individuals over time at farm scale sorted by pathogen and initial risk level proportion. HR30: 30%, 40% and 30% of low, medium, and high risk level respectively. HR10: 90% of low risk individuals and 10% of high risk. Homogeneous: all 10 batches have equal risk level proportions. Sorted: each one of the 10 batches is composed of only one risk level. Unique: there is only one batch.

scenarios only feature one batch, they were not included in the figure. No effect of sorting batches was observable for BRSV in HR30, as almost every batch was infected in every scenario.

### 3.3. Sensitivity analysis

The sensitivity analysis on every pathogen and scenarios HR30-sorted, HR30-homogeneous and HR30-unique showed that the probability of spontaneous shedding (*reactivation*, or  $p_E$ ) played a predominant role in the variation of all considered outputs for both bacteria while the variation of the outputs was mostly driven by the duration of the infectious period ( $dur_I$  or  $\tau_I$ ) for BRSV (Fig. 8). The parameter tuning the partial immunity of the I2 individuals also carried a non-negligible part of the variation of maximum number of infectious individuals for BRSV.

The variation of the proportion of medium risk carriers had a more important effect on the outputs than the variation of the proportion of high risk carriers for sorted scenarios. This was not observed in the homogeneous and unique scenarios.

The duration of the asymptomatic period appeared to play an important role in the average maximum number of detected cases for *M. bovis*. The contribution of this parameter to the variation of this output became predominant in the scenario with a unique batch. The variation of this parameter also contributed to the variation of the average AMU for *M. haemolytica*.

The variation of the detection sensitivity to mild clinical signs played a major role in the false negative rate for *M. haemolytica* in every scenario. It also impacted the variation of the average maximum number of detected for BRSV in the unique and homogeneous scenarios.

The variation of the individual sensitivities and transmission rates participated in the variation of the cumulative incidence and the AMU for both bacteria in every scenario. Additionally, medium risk sensitivity

and high risk transmission rate showed a non-negligible contribution to the variation of the height of the epidemic peak for BRSV in the unique scenario.

### 3.4. Interbatch contact rate

The farm-scale cumulative incidence increased with the contact rate between batches for BRSV and *M. bovis* up to a threshold, while staying globally constant for *M. haemolytica* (Fig. 9). For BRSV, under  $c = 0.02$ , the average cumulative incidence dropped by around 34% for homogeneous batches and 41% for sorted batches. We observed a similar effect for *M. bovis*, with a threshold around 0.1 and a drop of 18% for homogeneous batches and 38% for sorted batches. For *M. haemolytica*, the cumulative incidence remained lower for the sorted scenario than for the homogeneous.

The median number of batches with at least one case occurrence also increased with the contact rate up to a threshold for every pathogen and scenarios (Fig. 10). Moreover, we observed a threshold value for the contact rate, above which the number of batches with horizontal transmission stabilized. This threshold was around 0.05 for *M. haemolytica* in homogeneous batches and 0.08 in sorted batches. The threshold was also around 0.05 for *M. bovis* but was lower (around 0.01) for BRSV. Additionally, the number of batches with horizontal disease transmission was decreased in sorted batches scenario for both bacteria, especially when the contact rate between batches was low.

## 4. Discussion

This study aimed at modeling the impact of three batch allocation systems with two individual risk level proportions on the spread of three causal pathogens of BRD. We computed the cumulative incidence, the



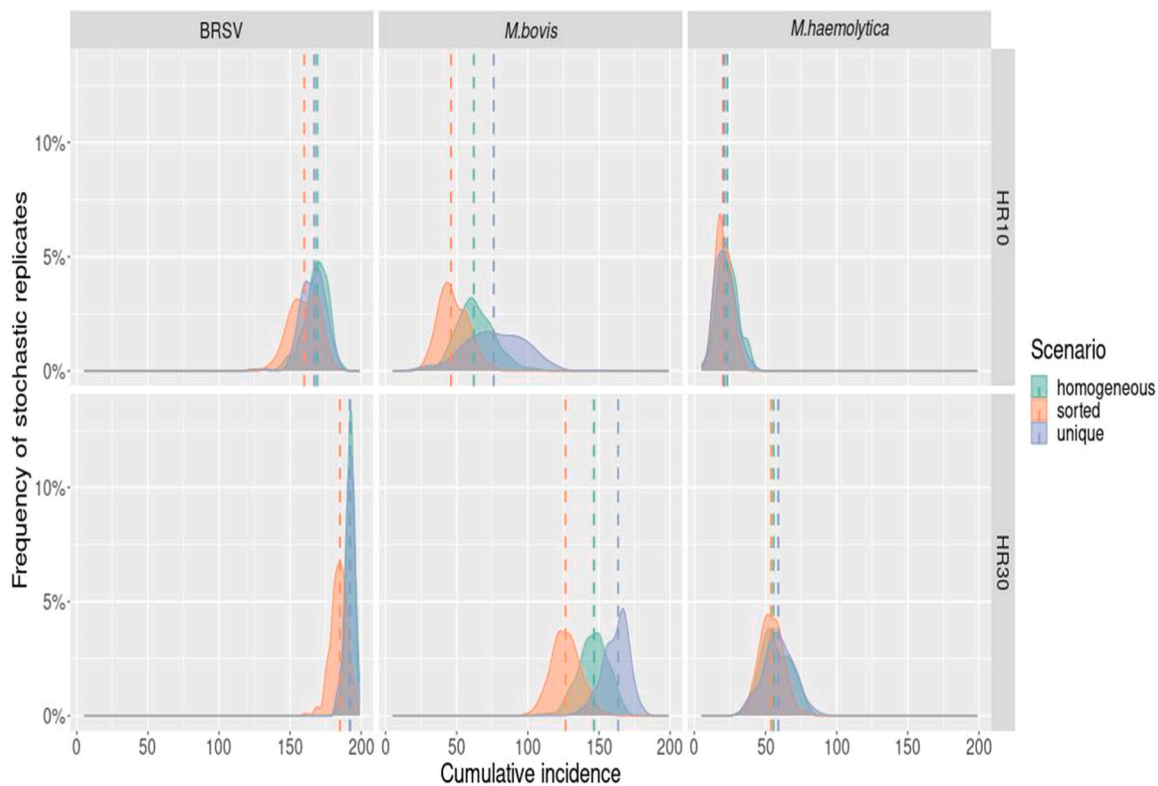


**Fig. 4.** Distributions of the cumulative incidence at farm scale for each pathogen and scenarios. HR30: 30%, 40% and 30% of low, medium, and high risk level respectively. HR10: 90% of low risk individuals and 10% of high risk. Homogeneous: all 10 batches have equal risk level proportions. Sorted: each one of the 10 batches is composed of only one risk level. Unique: there is only one batch.

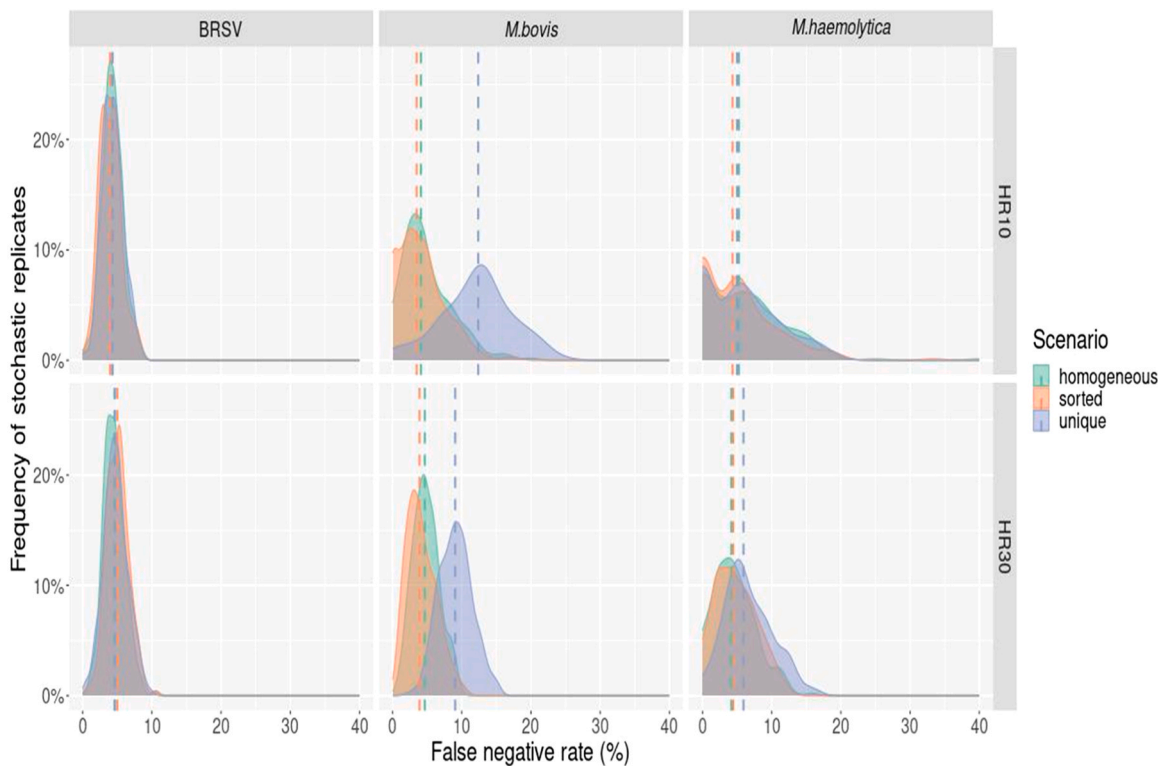


**Fig. 5.** Distributions of the false negative rate for each pathogen and scenarios. HR30: 30%, 40% and 30% of low, medium, and high risk level respectively. HR10: 90% of low risk individuals and 10% of high risk. Homogeneous: all 10 batches have equal risk level proportions. Sorted: each one of the 10 batches is composed of only one risk level. Unique: there is only one batch.

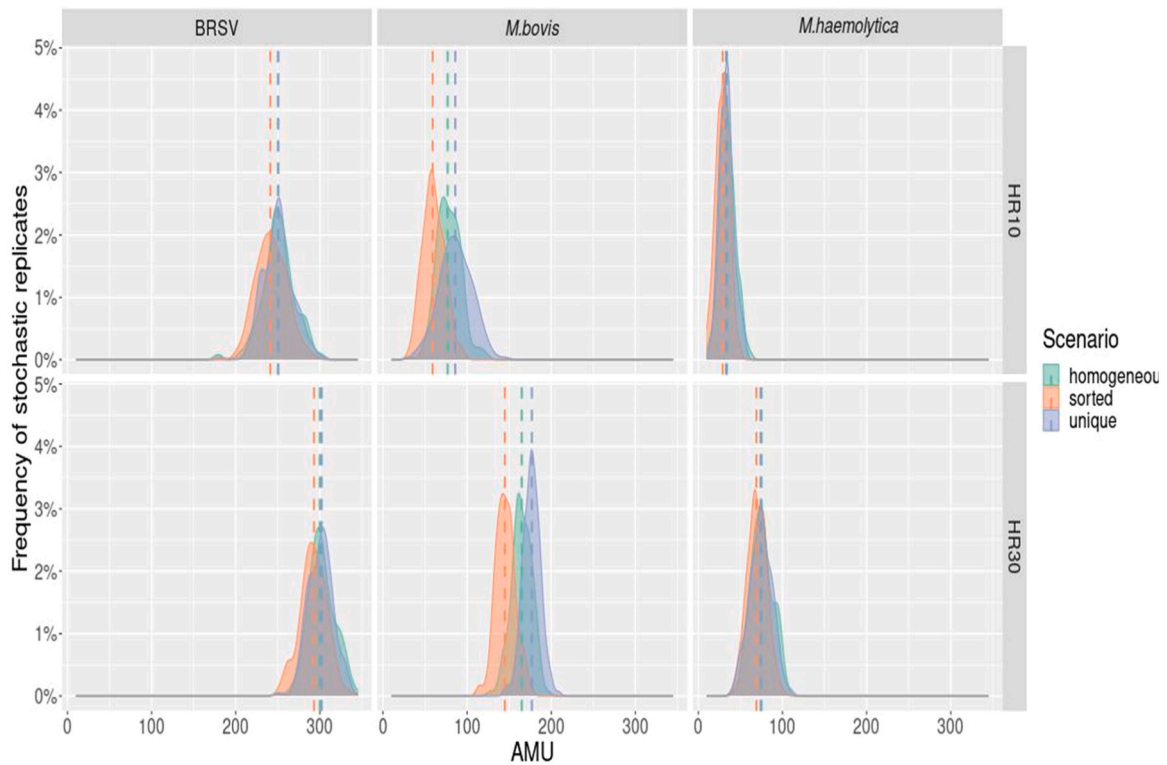


**Fig. 6.** Distributions of the AMU for each pathogen and scenarios. HR30: 30%, 40% and 30% of low, medium, and high risk level respectively. HR10: 90% of low risk individuals and 10% of high risk. Homogeneous: all 10 batches have equal risk level proportions. Sorted: each one of the 10 batches is composed of only one risk level. Unique: there is only one batch.

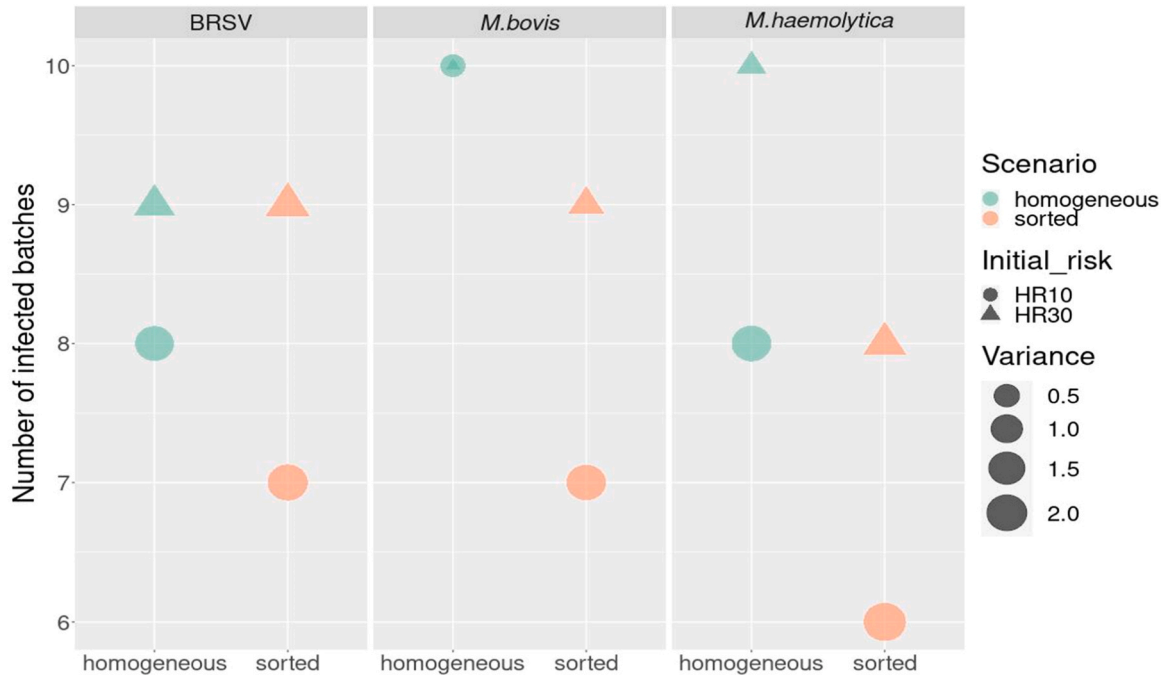


**Fig. 7.** Median number of infected batches for each pathogen and scenarios. HR30: 30%, 40% and 30% of low, medium, and high risk level respectively. HR10: 90% of low risk individuals and 10% of high risk. Homogeneous: all 10 batches have equal risk level proportions. Sorted: each one of the 10 batches is composed of only one risk level. Unique: there is only one batch.

height of the epidemic peak and the AMU for each pathogen in every scenario. We proposed that allocating animals in batches sorting them by risk levels could minimize case occurrence and AMU. Such information could impact the decision-making in the industry in terms of

animal purchase and farm management in cattle fattening farms.

We showed that managing a herd in smaller sorted batches tended to reduce the spread of BRSV, *M. haemolytica* and *M. bovis*. As underlined in modeling and quantitative field studies, larger batches tend to increase

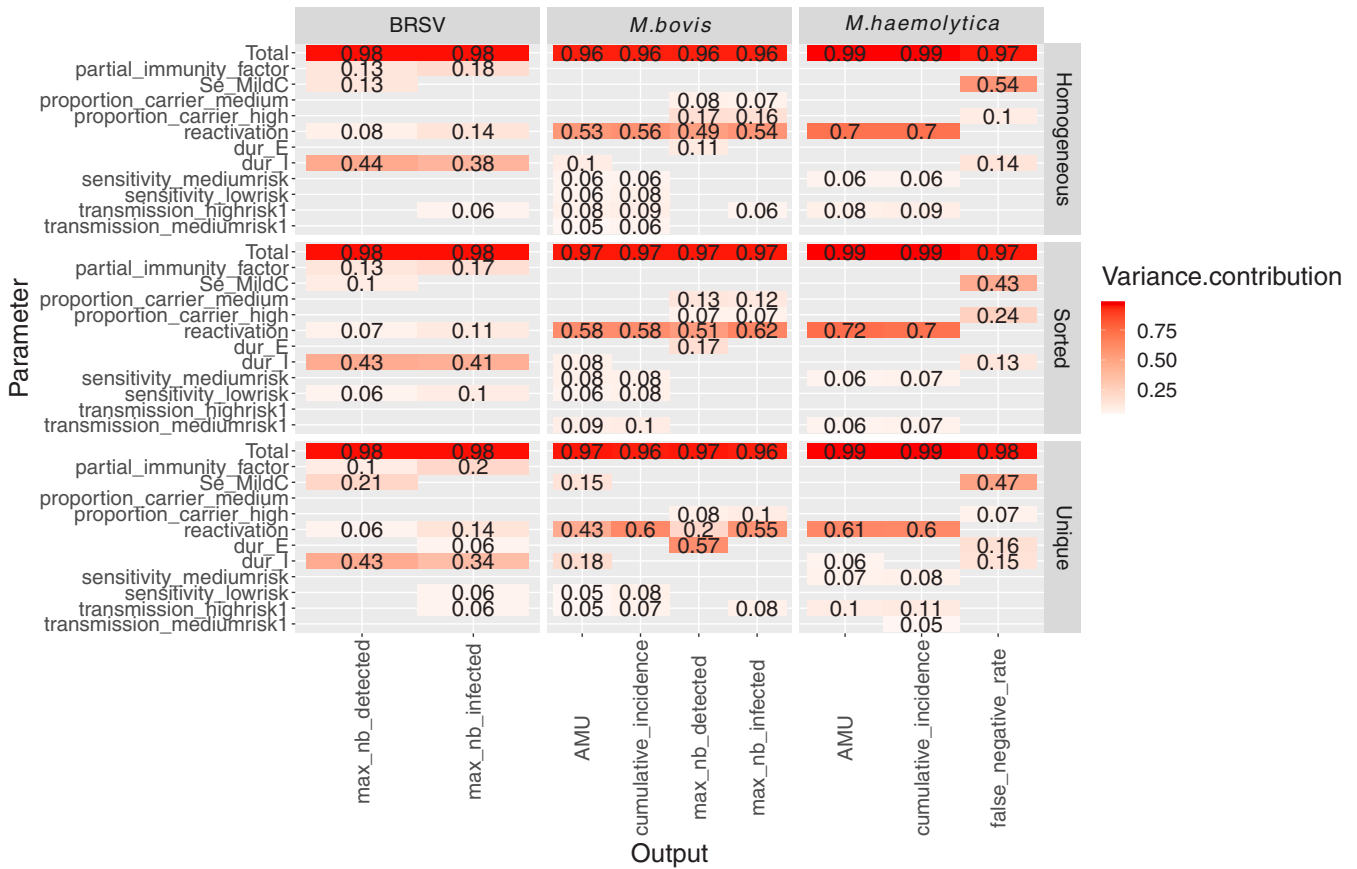


**Fig. 8.** Sensitivity analysis for 3 pathogens and 3 scenarios with 30%, 40% and 30% of low, medium, and high risk individuals respectively (HR30), we considered the following scenarios: homogeneous, sorted batches or unique batch. For each scenario, we display the contribution (total sensitivity index calculated by an ANOVA of each parameter (one per line) to the variation of target outputs (one per column). For each output (i.e. for each column), the numeric values represent the effect of the most impactful parameter. Contributions smaller than 0.05 are left out. Only the outputs with a normal distribution were analyzed.

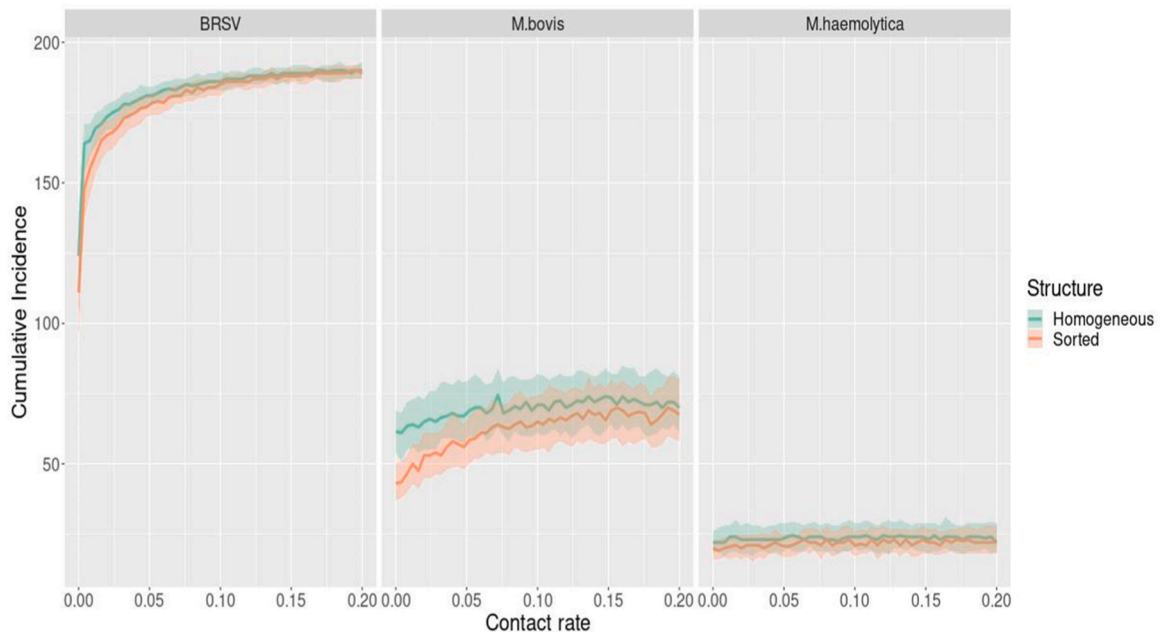


**Fig. 9.** Impact of the value of the interbatch *contact rate* on the cumulative incidence for each pathogen in a population with 90% of low risk individuals and 10% of high risk individuals (HR10). Homogeneous: every batch has the same risk level proportion. Sorted, 90% of the batches are only composed of low risk individuals and 10% are only composed of high risk individuals. The ribbon represents the 25% and 75% quantiles of the replicates while the solid line is the average value.

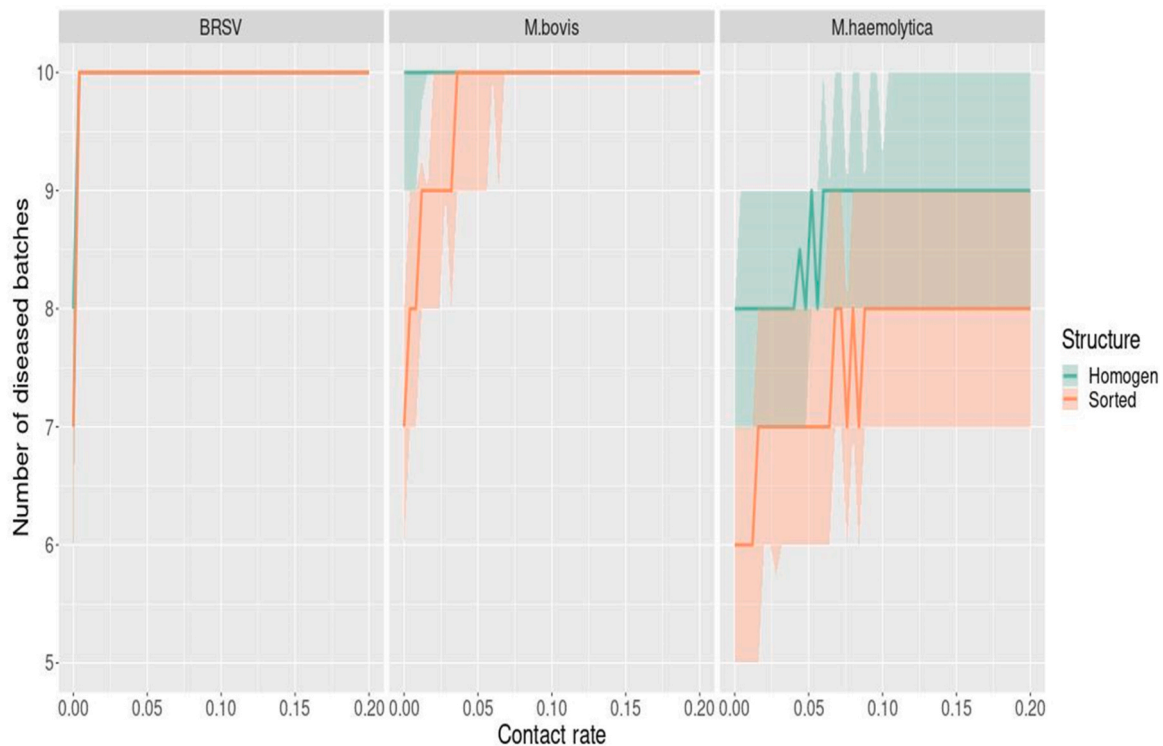


**Fig. 10.** Impact of the interbatch *contact rate* on the median number of batches with at least one infectious individual for each pathogen in a population with 90% of low risk individuals and 10% of high risk individuals. Homogeneous: every batch has equal risk level proportion. Sorted: 90% of the batches are only composed of low risk individuals and 10% are only composed of high risk individuals.

the risk of BRD (Ince et al., 2021; Picault et al., 2022). In other published research, higher prevalence of respiratory diseases can be found in larger groups of veal calves (Studer et al., 2021). We could thus expect several smaller pens to be a better option than a single large batch. For BRSV, this higher viral circulation was accompanied by shorter episodes, which was expected given how contagious this pathogen is and how few susceptible individuals were remaining after the epidemic peak. However, studies on BRSV yearly reinfections pointed towards a remnant circulation of BRSV among the already infected (Van der Poel et al., 1993; Norström et al., 2000). These results were obtained on dairy cows which have a different farming system. Nevertheless, a degree of low level steady reinfection could be of interest in a longer term model.

Our model also allowed us to assess the importance of batch composition on pathogen circulation at farm scale. Our results showed that reducing the proportion of high-risk individuals in the fattening farm successfully reduced the size of the epidemic peak as well as the persistence of the pathogen in the population. This finding is in agreement with results obtained in quantitative epidemiological studies (Norström et al., 2000; Herve et al., 2020). These authors highlighted that minimizing transportation and increasing vaccination yielded better cattle performances. In our model, individual risk levels (which represent qualitative information on risk factors for BRD) modulated pathogen prevalence as well as transmission rate and susceptibility. Hence, this was an expected finding. Similar conclusions were drawn out in Hay et al., where group heterogeneity and the distance traveled were proven to be risk factors for developing BRD (Hay et al., 2014). We built the model under the assumption that individual risk level influenced the susceptibility of the individuals, as well as their transmission rate in the event of their infection. In other words, a population with more high-risk individuals was more susceptible to infection and infectious animals were more likely to contaminate susceptible ones. The sensitivity analysis also indicated that one of the driving parameters of our model was the probability of spontaneously shedding pathogen. This particular parameter depended on the individual risk level. It thus confirmed the

impact of individual risk level on the epidemiological dynamics under the given assumptions.

Composing batches according to such individual risk levels tended to result in lower disease incidence for every pathogen, especially for *M. bovis*. This finding is consistent with a field study by Bach et al. where groups were formed according animals' previous BRD history (Bach et al., 2011). In this study, the proportion of calves infected increased according to the proportion of animals with BRD history. Minimizing the number of source farms for batch composition has also been shown to reduce the risk of a BRD outbreak (Morel-Journel et al., 2021). However, body weight heterogeneity was also proven to contribute to reducing the risk of outbreak (Herve et al., 2020). Such heterogeneity cannot be obtained by animals coming from the same breeder, as breeders tend to produce animals of homogeneous body weight. Therefore, there is a trade-off to consider at batch composition. Further data is needed to quantify this trade-off.

Furthermore, our results for AMU followed the same conclusions as cumulative incidence and pointed towards a reduction of the number of doses used in the sorted scenarios. Consistently, in Santinello et al., sorting high risk individuals apart from the herd (*i.e.* a quarantine) proved to be an efficient way to reduce the AMU (Santinello et al., 2022). Collective curative treatments and batch-scale preventive treatments were not included in our study but could possibly outline benefits of sorting batches to limit AMU, especially for low contact rate between batches.

The investigated scenarios had little impact on AMU for BRSV. Antimicrobials have no effect on BRD due to BRSV but treatment was kept anyway in the model, assuming that the involved pathogen was not identified before treatment and that AMU was the standard procedure in the event of clinical signs appraisal. AMU was therefore a mere reflection of BRSV spread. However, BRSV is known for being a primary pathogen often involved in bacterial superinfections (Matović et al., 2020; Gaudino et al., 2022). Further investigations should thus be conducted to assess the role of AMU on preventing these secondary

infections.

Finally, we explored the impact of the contact rate between batches on BRD incidence on farm and in specific batches. It appeared that when the contact is close to zero, the cumulative incidence drops significantly for BRSV and *M. bovis*. This effect had a greater amplitude when the batches were sorted. In that case, the most infectious individuals were in contact with fewer susceptible individuals and therefore could not infect them. The contact rate variations did not have any observable effects on the spread of *M. haemolytica*. This could be due to the fact that horizontal transmission is not the main driver of the spread of this pathogen. Indeed, the dynamics of *M. haemolytica* were mostly driven by carriage and therefore could be less impacted by a change in contact rate.

In conclusion, interesting operational perspectives arise from a pathogen-specific BRD model. We included BRSV, *M. bovis* and *M. haemolytica* in our study. The main findings were the reduction of the cumulative incidence for each of these agents. when the population was organized in multiple batches sorted by risk levels and the increase in the incidence and less sensitive case detection when the population was organized in a unique batch. A previous study highlighted that housing cattle according to BRD history reduces BRD occurrence at the group level (Bach et al., 2011). Our model further argues that housing cattle according to BRD risk factors and stressors could reduce BRD incidence and AMU, especially for long-time persisting agents such as *M. bovis*.

This model provides a solid basis for further models aiming to evaluate the effects of other intervention strategies, such as the implementation of alternative case detection methods or collective treatments. Future work could also test our recommendations in a model taking into account pathogen coinfections to assess their impact on these recommendations. Future models could benefit from more precise information or data on pathogen epidemiological dynamics. An adaptive contact rate could also be used to model the spatial distribution of individuals and its effects on pathogen circulation.

## Declaration of Competing Interest

The authors declare no conflicts of interest.

## Acknowledgements

This work has received funding from the European Union's Horizon 2020 research and innovation program under grant agreement No. 101000494 (DECIDE) and from the French region Pays de Loire. We thank our colleagues from the BIOEPAR Dynamo team for their comments and advice on this work. We are most grateful to the INRAE MIGALE bioinformatics facility (MIGALE, INRAE, 2020. Migale bioinformatics Facility " Migale platform | Migale ", s. d, for the use of their computing resources.

## Appendix A. Supporting information

Supplementary data associated with this article can be found in the online version at [doi:10.1016/j.prevetmed.2023.106009](https://doi.org/10.1016/j.prevetmed.2023.106009).

## References

- Amrine, David E., McLellan, Jiena G., White, Brad J., Larson, Robert L., Renter, David G., Sanderson, Mike, et al., 2019. Evaluation of three classification models to predict risk class of cattle cohorts developing bovine respiratory disease within the first 14 days on feed using on-arrival and/or pre-arrival information (janvier). *Comput. Electron. Agric.* 156, 439–446. <https://doi.org/10.1016/j.compag.2018.11.035>.
- Assié, S., Seegers, H., Makoschey, B., Désiré-Bousquié, L., Bareille, N., et al., 2009. Exposure to pathogens and incidence of respiratory disease in young bulls on their arrival at fattening operations in France. *Veterinary Rec.* 165 (7), 195–199. <https://doi.org/10.1136/vr.165.7.195>.
- Babcock, A.H., White, B.J., Dritz, S.S., Thomson, D.U., Renter, D.G., et al., 2009. " Feedlot health and performance effects associated with the timing of respiratory disease treatment. *J. Anim. Sci.* 87 (1), 314–327.
- Babcock, Abram H., White, Brad J., Renter, David G., Dubnicka, Suzanne R., Morgan Scott, H., et al., 2013. Predicting cumulative risk of bovine respiratory disease

- complex (BRDC) using feedlot arrival data and daily morbidity and mortality counts. *Can. J. Veterinary Res. = Rev. Can. De. Rech. Vet.* 77 (1), 33–44.
- Bach, A., Tejero, C., Ahedo, J., 2011. Effects of group composition on the incidence of respiratory afflictions in group-housed calves after weaning. *J. Dairy Sci.* 94 (4), 2001–2006. <https://doi.org/10.3168/jds.2010-3705>.
- Bareille, Nathalie, Seegers, Henri, Quillet, Jean-Michel, Assié, S., Bastien, et al., 2009. Impact of respiratory disorders in young bulls during their fattening period on performance and profitability. In 25. World Buiatrics Congr. 1–p.
- Blakebrough-Hall, Claudia, Hick, Paul, Mahony, T.J., González, Luciano A., et al., 2022. Factors associated with bovine respiratory disease case fatality in feedlot cattle. *J. Anim. Sci.* 100 (1), skab361. <https://doi.org/10.1093/jas/skab361>.
- Brodersen, Bruce W., 2010. Bovine respiratory syncytial virus. *Veterinary Clin. North Am.: Food Anim. Pract., Bov. Respir. Dis.* 26 (2), 323–333. <https://doi.org/10.1016/j.cvfa.2010.04.010>.
- Caswell, Jeff L., Bateman, Ken G., Cai, Hugh Y., Castillo-Alcala, Fernanda, et al., 2010. Mycoplasma bovis in respiratory disease of feedlot cattle. *Veterinary Clin.: Food Anim. Pract.* 26 (2), 365–379. <https://doi.org/10.1016/j.cvfa.2010.03.003>.
- Cernicchiaro, N., White, B.J., Renter, D.G., Babcock, A.H., Kelly, L., Slattery, R., 2012. Associations between the distance traveled from sale barns to commercial feedlots in the United States and overall performance, risk of respiratory disease, and cumulative mortality in feeder cattle during 1997 to 2009. *J. Anim. Sci.* 90 (6), 1929–1939. <https://doi.org/10.2527/jas.2011-4599>.
- Chase, Chris. 2021. Practical Immunology and Beef and Dairy vx Protocols: American Association of Bovine Practitioners Conference Proceedings, février, 10–18. <https://doi.org/10.21423/aabppro20218160>.
- Coetzee, Johann F., Magstadt, Drew R., Sidhu, Pritam K., Follett, Lendie, Schuler, Adlai M., Krull, Adam C., Cooper, Vickie L., Engelken, Terry J., Kleinhenz, Michael D., M O'Connor, Annette, 2019. Association between antimicrobial drug class for treatment and retreatment of bovine respiratory disease (BRD) and frequency of resistant BRD pathogen isolation from veterinary diagnostic laboratory samples. *PLoS One* 14 (12), e0219104.
- De Jong, M.C., van Oirschot, J.T., van der Poel, W.H., Kramps, J.A., Brand, A., 1996. Quantitative investigation of population persistence and recurrent outbreaks of bovine respiratory syncytial virus on dairy farms. *Am. J. Vet. Res.* 57 (5), 628–633.
- DeDonder, Keith D., Apley, Michael D., 2015. A review of the expected effects of antimicrobials in bovine respiratory disease treatment and control using outcomes from published randomized clinical trials with negative controls. *Veterinary Clin. North Am.: Food Anim. Pract., Bov. Clin. Pharmacol.* 31 (1), 97–111. <https://doi.org/10.1016/j.cvfa.2014.11.003>.
- Delabouglise, Alexis, Andrew James, Jean-François Valarcher, Sara Hagglund, Didier Rabaïsson, Jonathan Rushton. 2017. Linking Disease Epidemiology and Livestock Productivity: The Case of Bovine Respiratory Disease in France. Édité par Glenn F. Browning. PLOS ONE 12 (12): e0189090. <https://doi.org/10.1371/journal.pone.0189090>.
- Ellis, John A., Gow, Sheryl P., Mahan, Suman, Leyh, Randy, 2013. Duration of immunity to experimental infection with bovine respiratory syncytial virus following intranasal vaccination of young passively immune calves. *J. Am. Veterinary Med. Assoc.* 243 (11), 1602–1608. <https://doi.org/10.2460/javma.243.11.1602>.
- Ferguson, Neil M., Cummings, Derek A.T., Cauchemez, Simon, Fraser, Christophe, Riley, Steven, Meeyai, Aronrag, Iamsirithaworn, Sophon, Burke, Donald S., et al., 2005. Strategies for containing an emerging influenza pandemic in Southeast Asia. *Nature* 437 (7056), 209–214. <https://doi.org/10.1038/nature04017>.
- Frank, G.H., Briggs, R.E., Gillette, K.G., 1986. Colonization of the nasal passages of calves with *Pasteurella haemolytica* serotype 1 and regeneration of colonization after experimentally induced viral infection of the respiratory tract. *Am. J. Veterinary Res.* 47 (8), 1704–1707.
- Gaudino, Maria, Nagamine, Brandy, Ducatez, Mariette F., Meyer, Gilles, et al., 2022. Understanding the mechanisms of viral and bacterial coinfections in bovine respiratory disease: a comprehensive literature review of experimental evidence. *Veterinary Res.* 53 (1), 70. <https://doi.org/10.1186/s13567-022-01086-1>.
- Gershwin, Laurel J., Van Eenennaam, Alison L., Anderson, Mark L., McEligot, Heather A., Shao, Matt X., Toaff-Rosenstein, Rachel, Taylor, Jeremy F., Neiberger, Holly L., Womack, James, Bovine Respiratory Disease Complex Coordinated Agricultural Project Research Team, et al., 2015. Single pathogen challenge with agents of the bovine respiratory disease complex. édité par Kevin Harrod. PLOS ONE 10 (11), e0142479. <https://doi.org/10.1371/journal.pone.0142479>.
- Greenhalgh, David, Griffiths, Martin, et al., 2009. Backward bifurcation, equilibrium and stability phenomena in a three-stage extended BRSV epidemic model. *J. Math. Biol.* 59 (1), 1–36.
- Griffin, Dee, 2010. Bovine pasteurellosis and other bacterial infections of the respiratory tract. *Veterinary Clin. North Am.: Food Anim. Pract.* 26 (1), 57–71. <https://doi.org/10.1016/j.cvfa.2009.10.010>.
- Griffin, Dee, 2014. The monster we don't see: subclinical BRD in beef cattle. *Anim. Health Res. Rev.* 15 (2), 138–141.
- Grissett, G.P., White, B.J., Larson, R.L., 2015. Structured literature review of responses of cattle to viral and bacterial pathogens causing bovine respiratory disease complex. *J. Veterinary Intern. Med.* 29 (3), 770–780. <https://doi.org/10.1111/jvim.12597>.
- Hall, Caroline Breese, Walsh, Edward E., Long, Christine E., Schnabel, Kenneth C., 1991. Immunity to and Frequency of Reinfection with Respiratory Syncytial Virus. *J. Infect. Dis.* 163 (4), 693–698. <https://doi.org/10.1093/infdis/163.4.693>.
- Hay, K.E., Barnes, T.S., Morton, J.M., Clements, A.C.A., Mahony, T.J., et al., 2014. Risk factors for bovine respiratory disease in Australian Feedlot cattle: use of a causal diagram-informed approach to estimate effects of animal mixing and movements before feedlot entry. *Prev. Veterinary Med.* 117 (1), 160–169. <https://doi.org/10.1016/j.prevetmed.2014.07.001>.

- Hay, K.E., Morton, J.M., Schibrowski, M.L., Clements, A.C.A., Mahony, T.J., Barnes, T.S., et al., 2016. Associations between prior management of cattle and risk of bovine respiratory disease in feedlot cattle (mai). *Prev. Veterinary Med.* 127, 37–43. <https://doi.org/10.1016/j.prevetmed.2016.02.006>.
- Herve, Lucile, Bareille, Nathalie, Cornette, Baptiste, Loiseau, Pauline, Assié, S.ébastien, 2020. To what extent does the composition of batches formed at the sorting facility influence the subsequent growth performance of young beef bulls? A french observational study (mars). *Prev. Veterinary Med.* 176, 104936. <https://doi.org/10.1016/j.prevetmed.2020.104936>.
- Hilton, W.Mark, 2014. BRD in 2014: where have we been, where are we now, and where do we want to go? *Anim. Health Res. Rev.* 15 (2), 120–122. <https://doi.org/10.1017/S1466252314000115>.
- İnce, Ömer Bari.ş., Şevik, Murat, Özgür, Emrah G.ökay, Sait, Ahmet, et al., 2021. Risk factors and genetic characterization of bovine respiratory syncytial virus in the Inner Aegean Region, Turkey. *Trop. Anim. Health Prod.* 54 (1), 4. <https://doi.org/10.1007/s11250-021-03022-5>.
- Ives, Samuel E., Richeson, John T., et al., 2015. Use of antimicrobial metaphylaxis for the control of bovine respiratory disease in high-risk cattle (v). *Veterinary Clin. North Am. Food Anim. Pract.* 31 (3), 341–350. <https://doi.org/10.1016/j.cvfa.2015.05.008>.
- Kayser, William C., Carstens, Gordon E., Jackson, Kirby S., Pinchak, William E., Banerjee, Amarnath, Fu, Yu, et al., 2019. Evaluation of statistical process control procedures to monitor feeding behavior patterns and detect onset of bovine respiratory disease in growing bulls. *J. Anim. Sci.* 97 (3), 1158–1170. <https://doi.org/10.1093/jas/sky486>.
- Keeling, Matt, 2005. The implications of network structure for epidemic dynamics. *Theor. Popul. Biol.* 67 (1), 1–8. <https://doi.org/10.1016/j.tpb.2004.08.002>.
- Klem, Thea Blystad, Sjørseth, Siri Kulberg, Sviland, Ståle, Gjerset, Britt, Myrmed, Mette, Stokstad, Maria, et al., 2019. Bovine respiratory syncytial virus in experimentally exposed and rechallenged calves; viral shedding related to clinical signs and the potential for transmission. *BMC Veterinary Res.* 15 (1), 156. <https://doi.org/10.1186/s12917-019-1911-z>.
- Kobilinsky, André, Monod, Hervé, Bailey, R.A., et al., 2017. Automatic generation of generalised regular factorial designs (septembre). *Comput. Stat. Data Anal.* 113, 311–329. <https://doi.org/10.1016/j.csda.2016.09.003>.
- Kudirkienė, Eglė, Aagaard, Anne Katrine, Schmidt, Louise M.B., Pansri, Potjamas, Krogh, Kenneth M., Olsen, John E., et al., 2021. Occurrence of major and minor pathogens in calves diagnosed with bovine respiratory disease. *Veterinary Microbiol.* 259 (août), 109135. <https://doi.org/10.1016/j.vetmic.2021.109135>.
- Laxminarayan, Ramanan, Duse, Adriano, Wattal, Chand, Zaidi, Anita K.M., Wertheim, Heiman F.L., Sumpredit, Nithima, Vlieghe, Erika, et al., 2013. Antibiotic resistance—the need for global solutions. *Lancet Infect. Dis.* 13 (12), 1057–1098.
- Le Grand, Dominique, Arcangioli, Marie-Anne, Calavas, Didier, Bézille, Pierre, Poumarat, François, et al., 2008. Mycoplasmes et mycoplasmoses bovines: actualités. *Bull. De l'Académie vétérinaire De. Fr.* 161 (2), 159–166.
- Matović, Kazimir, Vladimir Kurčić, Radojica Đoković, Miloš, Petrović, Milanko Šekler, Bojana Tešović et al. 2020. Paradigm of coinfection with viral and bacterial agents causing bovine respiratory disease complex (BRDC) in Central Serbia. <https://doi.org/10.5937/AASer2049083M>.
- " Migale platform | Migale ". s. d. Consulté le 2 février 2023. <https://migale.inrae.fr/>.
- Mijar, Sanjaya, van der Meer, Frank, Pajor, Ed, Hodder, Abigail, Morgan Louden, Julia, Thompson, Sean, Orsel, Karin, et al., 2023. Impacts of commingling preconditioned and auction-derived beef calves on bovine respiratory disease related morbidity, mortality, and weight gain. *Frontiers in Veterinary Science*, p. 10 <https://www.frontiersin.org/articles/10.3389/fvets.2023.1137078>.
- Morel-Journel, Thibaut, Assié, S.ébastien, Vergu, Elisabeta, Mercier, Jean-Baptiste, Bonnet-Beaugrand, Florence, Ezanno, Pauline, et al., 2021. Minimizing the number of origins in batches of weaned calves to reduce their risks of developing bovine respiratory diseases. *Veterinary Res.* 52 (1), 5. <https://doi.org/10.1186/s13567-020-00872-z>.
- Nobrega, Diego, Andres-Lasheras, Sara, Zaheer, Rahat, McAllister, Tim, Homerosky, Elizabeth, Michele Anholt, R., Dorin, Craig, et al., 2021. Prevalence, risk factors, and antimicrobial resistance profile of respiratory pathogens isolated from suckling beef calves to reprocessing at the feedlot: a longitudinal study. *Front. Veterinary Sci.* 8 <https://www.frontiersin.org/article/10.3389/fvets.2021.764701>.
- Norström, Madelaine, Skjerve, Eystein, Jarp, Jorun, et al., 2000. Risk factors for epidemic respiratory disease in Norwegian cattle herds. *Prev. Veterinary Med.* 44 (1), 87–96. [https://doi.org/10.1016/S0167-5877\(99\)00113-0](https://doi.org/10.1016/S0167-5877(99)00113-0).
- Ollivett, T.L., 2020. BRD treatment failure: clinical and pathologic considerations. *Anim. Health Res. Rev.* 21 (2), 175–176.
- Picault, S.ébastien, Pauline Ezanno, S.ébastien Assié et al. 2019. Combining early hyperthermia detection with metaphylaxis for reducing antibiotics usage in newly received beef bulls at fattening operations: a simulation-based approach ". In *SVEPM: Conference & Annual General Meeting*, 148–59.
- Picault, S.ébastien, Huang, Yu-Lin, Sicard, Vianney, Arnoux, Sandie, Beaunée, Gaël, Ezanno, Pauline, et al., 2019. EMULSION: transparent and flexible multiscale stochastic models in human, animal and plant epidemiology. *PLoS Comput. Biol.* 15 (9), e1007342.
- Picault, S.ébastien, Ezanno, Pauline, Smith, Kristen, Amrine, David, White, Brad, Assié, S.ébastien, et al., 2022. Modelling the effects of antimicrobial metaphylaxis and pen size on bovine respiratory disease in high and low risk fattening cattle. *Veterinary Res.* 53 (1), 77. <https://doi.org/10.1186/s13567-022-01094-1>.
- Poizat, Axelle, Duvaleix-Treguer, Sabine, Rault, Arnaud, Bonnet-Beaugrand, Florence, 2019. Le marché des brouards en France. Organisation de la filière, transmission de l'information et qualité (juin). *Économie Rural. Agric., Aliment., Territ. n° 368*, 107–127. <https://doi.org/10.4000/economierurale.6814>.
- Sacco, R.E., McGill, J.L., Pillatzki, A.E., Palmer, M.V., Ackermann, M.R., et al., 2014. Respiratory syncytial virus infection in cattle. *Veterinary Pathol.* 51 (2), 427–436. <https://doi.org/10.1177/0300985813501341>.
- Saltelli, Andrea, Annoni, Paola, Azzini, Ivano, Campolongo, Francesca, Ratto, Marco, Tarantola, Stefano, et al., 2010. Variance based sensitivity analysis of model output design and estimator for the total sensitivity index. *Comput. Phys. Commun.* 181 (2), 259–270. <https://doi.org/10.1016/j.cpc.2009.09.018>.
- Santiniello, Matteo, Diana, Alessia, De Marchi, Massimo, Scali, Federico, Bertocchi, Luigi, Lorenzi, Valentina, Loris Alborali, Giovanni, Penasa, Mauro, 2022. Promoting judicious antimicrobial use in beef production: the role of quarantine. *Animals* 12 (1), 116. <https://doi.org/10.3390/ani12010116>.
- Sharma, R., Woldehiwet, Z., 1992. Reinfection of Lambs with Bovine Respiratory Syncytial Virus. *Veterinary Sci.* 52 (1), 72–77. [https://doi.org/10.1016/0034-5288\(92\)90061-6](https://doi.org/10.1016/0034-5288(92)90061-6).
- Studer, Eveline, Schönecker, Lutz, Meylan, Mireille, Stucki, Dimitri, Dijkman, Ronald, Holwerda, Melle, Glaus, Anna, Becker, Jens, et al., 2021. Prevalence of BRD-related viral pathogens in the upper respiratory tract of swiss veal calves. *Animals* 11 (7), 1940. <https://doi.org/10.3390/ani11071940>.
- Thomas, A.C., Bailey, M., Lee, M.R.F., Mead, A., Morales-Aza, B., Reynolds, R., Vipond, B., Finn, A., Eisler, M.C., 2019. Insights into Pasteurellaceae carriage dynamics in the nasal passages of healthy beef calves. *Sci. Rep.* 9 (août), 11943. <https://doi.org/10.1038/s41598-019-48007-5>.
- Timsit, E., Christensen, H., Bareille, N., Seegers, H., Bisgaard, M., Assié, S., 2013. Transmission dynamics of mannheimia haemolytica in newly-received beef bulls at fattening operations. *Veterinary Microbiol.* 161 (3–4), 295–304. <https://doi.org/10.1016/j.vetmic.2012.07.044>.
- Timsit, Edouard, Assié, S.ébastien, Quiniou, René, Seegers, Henri, Bareille, Nathalie, et al., 2011. Early Detection of Bovine Respiratory Disease in Young Bulls Using Reticulo-Rumen Temperature Boluses. *Veterinary J.* 190 (1), 136–142. <https://doi.org/10.1016/j.tvjl.2010.09.012>.
- Tjørnehøj, K., Uttenhal, Å., Viuff, B., Larsen, L.E., Røntved, C., Rønsholt, L., 2003. An experimental infection model for reproduction of calf pneumonia with bovine respiratory syncytial virus (BRSV) based on one combined exposure of calves. *Res. Veterinary Sci.* 74 (1), 55–65. [https://doi.org/10.1016/S0034-5288\(02\)00154-6](https://doi.org/10.1016/S0034-5288(02)00154-6).
- Van der Poel, W.H.M., Kramps, J.A., Middel, W.G.J., Van Oirschot, J.T., Brand, A., et al., 1993. Dynamics of bovine respiratory syncytial virus infections: a longitudinal epidemiological study in dairy herds. *Arch. Virol.* 133 (3), 309–321. <https://doi.org/10.1007/BF01313771>.
- White, Brad J., Anderson, David E., Renter, David G., Larson, Robert L., Mosier, Derek A., Kelly, Lindsey L., Theurer, Miles E., Robért, Brad D., Walz, Michelle L., et al., 2012. Clinical, behavioral, and pulmonary changes in calves following inoculation with mycoplasma bovis. *Am. J. Veterinary Res.* 73 (4), 490–497. <https://doi.org/10.2460/ajvr.73.4.490>.
- Wolff, Cecilia, Emanuelson, Ulf, Ohlson, Anna, Alenius, Stefan, Fall, Nils, et al., 2015. Bovine respiratory syncytial virus and bovine coronavirus in swedish organic and conventional dairy herds. *Acta Veterinaria Scand.* 57 (1), 2. <https://doi.org/10.1186/s13028-014-0091-x>.